Nonsymmetrized hyperspherical harmonic basis for an A-body system

M. Gattobigio,[1,*] A. Kievsky,[2] and M. Viviani[2]

[1]*Université de Nice-Sophia Antipolis, Institut Non-Linéaire de Nice, CNRS, 1361 route des Lucioles, F-06560 Valbonne, France*

[2]*Istituto Nazionale di Fisica Nucleare, Largo Pontecorvo 3, I-56100 Pisa, Italy*

(Received 17 September 2010; published 9 February 2011)

The use of the hyperspherical harmonic (HH) basis in the description of bound states in an A-body system composed of identical particles is normally preceded by a symmetrization procedure in which the statistic of the system is taken into account. This preliminary step is not strictly necessary; the direct use of the HH basis is possible, even if the basis does not have a well-defined behavior under particle permutations. In fact, after the diagonalization of the Hamiltonian matrix, the eigenvectors reflect the symmetries present in it. They have well-defined symmetry under particle permutation and identification of the physical states is possible, as shown here in specific cases. The problem related to the large degeneration of the basis is circumvented by constructing the Hamiltonian matrix as a sum of products of sparse matrices. This particular representation of the Hamiltonian is well suited for a numerical iterative diagonalization, where only the action of the matrix on a vector is needed. As an example we compute bound states for systems with $A = 3$–6 particles interacting through a short-range central interaction. We also consider the case in which the potential is restricted to act in relative s waves with and without the inclusion of the Coulomb potential. This very simple model predicts results in qualitative good agreement with the experimental data and it represents the first step in a project dedicated to the use of the HH basis to describe bound and low-energy scattering states in light nuclei.

DOI: 10.1103/PhysRevC.83.024001 PACS number(s): 31.15.xj, 03.65.Ge, 21.45.−v, 36.40.−c

I. INTRODUCTION

The *ab initio* description of light nuclear systems, starting from the nucleon-nucleon (NN) interaction, requires well-established methods to solve the Schrödinger equation. Among them, the Green function Monte Carlo (GFMC) method has been extensively used to describe light nuclei up to $A = 10$, and the no-core shell model (NCSM) up to $A = 12$ [1,2]. In the $A \leqslant 4$ systems, well-established methods for treating both bound and scattering states exist, such as the Faddeev equations ($A = 3$) and the Faddeev-Yakubovsky equations ($A = 4$) in configuration or momentum space and the hyperspherical harmonic (HH) expansion. All these methods have proven to be of great accuracy and they have been tested using different benchmarks [3–5].

The HH method provides a systematic way of constructing a complete basis for expansion of the A-particle wave function, and its use in $A > 4$ systems has been the subject of intense investigations over recent years. In the specific case of application to nuclear physics, the wave function has to be antisymmetric, and therefore, the HH basis has been rearranged to produce basis states having well-defined properties under particle permutations. Different schemes to construct hyperspherical functions with an arbitrary permutational symmetry are given in Refs. [6–8]. Procedures for constructing HH functions in terms of a single-particle basis have been proposed in Refs. [9] and [10].

In a different approach, the authors have used the HH basis, without a previous symmetrization procedure, to describe bound states in three- and four-particle systems [11]. It has been observed that the eigenvectors of the Hamiltonian matrix reflect the symmetries present in it, even if it has been constructed using a nonsymmetrized basis. The only requirement was to include all the HH basis elements having the same grand angular quantum number K. It is a property of the HH basis that basis elements having well-defined behavior under particle permutation can be constructed as a linear combination of HH elements having the same value of K. Therefore, if the Hamiltonian commutes with the group of permutations of A objects, S_A, the diagonalization procedure generates eigenvectors having a well-defined permutation symmetry that can be organized in accordance with the irreducible representations of S_A. Moreover, after identification of those eigenvectors with the desired symmetry, the corresponding energies can be considered variational estimates. In particular, in Ref. [11], it was possible to identify a subset of eigenvectors and eigenvalues corresponding exactly to those that would be obtained performing a preliminary symmetrization of the states. It should be noted that the simplicity of using the HH basis without a preliminary antisymmetrization step has to be counterbalanced with the large dimension of the matrices to be diagonalized. However, at present, different techniques are available for solving (at least partially) this problem.

In the present article we continue the study of the nonsymmetrized HH basis, extending the applications to systems with $A > 4$. In pursuit of this goal, we have developed a particular representation of the Hamiltonian matrix, which is systematic with respect to the number of particles and well suited for a numerical implementation. As mentioned, one of the main problems in using the HH basis is its large degeneracy, resulting in very large matrices. In contrast, the potential energy matrix, expressed as a sum of pairwise interactions, cannot connect arbitrary basis elements differing

*mario.gattobigio@inln.cnrs.fr

in some specific quantum numbers. This means that in some representations each pairwise-interaction term has to be represented by a sparse matrix. For example, the matrix representation of the potential $V(1,2)$, constructed in terms of basis elements in which the quantum numbers of particles $(1,2)$ are well defined, is sparse in $A \geqslant 3$ systems. In fact, its matrix elements connecting basis elements with different quantum numbers labeling states that do not involve particles $(1,2)$ are zero. A problem arises when the matrix elements of the generic term $V(i,j)$, defining the interaction between particles (i,j), has to be calculated using basis elements in which the quantum numbers of particles (i,j) are not well defined. One operative way to solve this problem consists in rotating the basis to a system of coordinates in which particles (i,j) have well-defined quantum numbers. This makes the matrix $V(i,j)$ sparse. However, we would like the rotation matrix to be sparse too, which in general is not true. This last problem is solved by noting that the rotation matrix can be expressed as a product of sparse matrices, each one representing a rotation that involves a permutation of particles of successive numbering. After these manipulations the potential energy matrix results in a sum of products of sparse matrices suitable for numerical implementations.

The nuclear force strongly depends on the spatial, spin, and isospin relative states of the nucleons. Accordingly, different angular, spin, and isospin components having total angular momentum L, total spin S, and total isospin T appear in the wave function. Moreover, the wave function of the system being completely antisymmetric, different spatial symmetries can be formed. For example, the three-nucleon bound state is a $J^\pi = 1/2^+$ state and its wave function has $L = 0, 1, 2$, $S = 1/2, 3/2$, and $T = 1/2, 3/2$ and include symmetric, antisymmetric, and mixed spatial components. The four-nucleon bound state is a $J = 0^+$ state and its wave function has $L = 0, 1, 2$, $S = 0, 1, 2$, and $T = 0, 1, 2$ and includes symmetric, antisymmetric, and the two mixed spatial components. In both cases, considering all these possible angular momentum, spin, and isospin values, the number of HH states having well-defined spatial symmetries necessary to construct the complete wave function is equivalent to that of the nonsymmetrized basis (for a discussion of the $A = 4$ system see Ref. [13]). For $A > 4$ not all the possible spatial symmetries could be entered in the construction of the total wave function; however, in the cases studied in the present work, corresponding to $A = 5, 6$, the number of nonsymmetrized basis elements remains comparable to that of symmetrized elements. As an example we show results for $A = 3$–6 systems using short-range central interactions with and without the inclusion of the Coulomb potential.

To summarize, in this paper we present the implementation of the nonsymmetrized HH basis for an A-body system using the factorization of the potential energy matrix mentioned before. To give a detailed description of this construction, we consider only spatial degrees of freedom; accordingly, we show examples using a central interaction. The diagonalization of the Hamiltonian produces eigenvectors organized in multiplets of the dimension of the corresponding irreducible representation of S_A, and the different symmetries are identified using the appropriate Casimir operator. Not all the states belonging to a particular representation can be antisymmetrized using the spin-isospin functions of A nucleons, and therefore, these states are not physical. It should be noted that the physical states can appear in very high positions in the spectrum; this is particularly the case for $A > 4$ systems. In contrast, iterative methods, such as the Lanczos method, used to search selected eigenvalues and eigenvectors of large matrices are more efficient for extreme ones. In this respect, we have found it very convenient to use the symmetry-adapted Lanczos method proposed in Ref. [14], which restricts the search to states having a particular symmetry. When possible, comparisons to different results in the literature are made. Because we have in mind the description of light nuclear systems using realistic interactions, this study can be considered a preliminary step in the use of this technique.

The paper is organized as follows: Section II is devoted to a brief description of the HH basis. In Sec. III the expression for the potential energy matrix in terms of HH states is given. In Sec. IV the results for the models proposed are shown. Section V includes a brief discussion of the results and the perspectives of the present work.

II. THE HARMONIC HYPERSPHERICAL BASIS FOR A BODIES

In this section we introduce the notation and we present a brief overview of the properties of the HH basis.

A. Basic properties of the HH basis

In accord with Ref. [11], we start with the following definition of the Jacobi coordinates for an A-body system with Cartesian coordinates $\mathbf{r}_1 \ldots \mathbf{r}_A$:

$$\mathbf{x}_{N-j+1} = \sqrt{\frac{2m_{j+1}M_j}{(m_{j+1}+M_j)m}}\,(\mathbf{r}_{j+1} - \mathbf{X}_j), \quad j = 1, \ldots, N, \tag{1}$$

where m is a reference mass, $N = A - 1$, and where we have defined

$$M_j = \sum_{i=1}^{j} m_i, \quad \mathbf{X}_j = \frac{1}{M_j}\sum_{i=1}^{j} m_i \mathbf{r}_i. \tag{2}$$

Let us note that if all the masses are equal, $m_i = m$, Eq. (1) simplifies to

$$\mathbf{x}_{N-j+1} = \sqrt{\frac{2j}{j+1}}\,(\mathbf{r}_{j+1} - \mathbf{X}_j), \quad j = 1, \ldots, N. \tag{3}$$

For a given set of Jacobi coordinates $\mathbf{x}_1, \ldots, \mathbf{x}_N$, we can introduce the hyper-radius ρ,

$$\rho = \left(\sum_{i=1}^{N} x_i^2\right)^{1/2} = \left(2\sum_{i=1}^{A}(\mathbf{r}_i - \mathbf{X})^2\right)^{1/2} = \left(\frac{2}{A}\sum_{j>i}^{A}(\mathbf{r}_j - \mathbf{r}_i)^2\right)^{1/2}, \tag{4}$$

and the hyperangular coordinates Ω_N,

$$\Omega_N = (\hat{\boldsymbol{x}}_1, \ldots, \hat{\boldsymbol{x}}_N, \phi_2, \ldots, \phi_N), \tag{5}$$

with the hyperangles ϕ_i defined via

$$\cos\phi_i = \frac{x_i}{\sqrt{x_1^2 + \cdots + x_i^2}}, \quad i = 2, \ldots, N. \tag{6}$$

The radial components of the Jacobi coordinates can be expressed in terms of the hyperspherical coordinates

$$\begin{aligned} x_N &= \rho\cos\phi_N, \\ x_{N-1} &= \rho\sin\phi_N\cos\phi_{N-1}, \\ &\vdots \\ x_i &= \rho\sin\phi_N\cdots\sin\phi_{i+1}\cos\phi_i, \\ &\vdots \\ x_2 &= \rho\sin\phi_N\cdots\sin\phi_3\cos\phi_2, \\ x_1 &= \rho\sin\phi_N\cdots\sin\phi_3\sin\phi_2. \end{aligned} \tag{7}$$

Using the preceding hyperspherical angles Ω_N and the angles (φ_i, θ_i) defining the direction of the unit Jacobi vector $\hat{\boldsymbol{x}}_i$, the surface element becomes

$$\begin{aligned} d\Omega_N = {} & \sin\theta_1\, d\theta_1\, d\varphi_1 \prod_{j=2}^{N} \sin\theta_j\, d\theta_j\, d\varphi_j (\cos\phi_j)^2 \\ & \times (\sin\phi_j)^{3j-4} d\phi_j\,, \end{aligned} \tag{8}$$

and the Laplacian operator

$$\Delta = \sum_{i=1}^{N} \nabla_{\mathbf{x}_i}^2 = \left(\frac{\partial^2}{\partial\rho^2} + \frac{3N-1}{\rho}\frac{\partial}{\partial\rho} + \frac{\Lambda_N^2(\Omega_N)}{\rho^2} \right), \tag{9}$$

where $\Lambda_N^2(\Omega_N)$ is the generalization of the angular momentum and is called the grand angular operator.

The HH functions $\mathcal{Y}_{[K]}(\Omega_N)$ are the eigenvectors of the grand angular momentum operator

$$\big(\Lambda_N^2(\Omega_N) + K(K+3N-2)\big)\mathcal{Y}_{[K]}(\Omega_N) = 0. \tag{10}$$

They can be expressed in terms of the usual harmonic functions $Y_{lm}(\hat{\boldsymbol{x}})$ and of the Jacobi polynomials $P_n^{a,b}(z)$. In fact, the explicit expression for the HH functions is

$$\mathcal{Y}_{[K]}(\Omega_N) = \left[\prod_{j=1}^{N} Y_{l_j m_j}(\hat{\boldsymbol{x}}_j) \right] \left[\prod_{j=2}^{N} {}^{(j)}\mathcal{P}_{K_j}^{\alpha_{l_j},\alpha_{K_{j-1}}}(\phi_j) \right], \tag{11}$$

where $[K]$ stands for the set of quantum numbers $l_1, \ldots, l_N, m_1, \ldots, m_N, n_2, \ldots, n_N$, and the hyperspherical polynomial is

$$\begin{aligned} & {}^{(j)}\mathcal{P}_{K_j}^{\alpha_{l_j},\alpha_{K_{j-1}}}(\phi_j) \\ & \quad = \mathcal{N}_{n_j}^{\alpha_{l_j},\alpha_{K_j}} (\cos\phi_j)^{l_j} (\sin\phi_j)^{K_{j-1}} P_{n_j}^{\alpha_{K_{j-1}},\alpha_{l_j}}(\cos 2\phi_j), \end{aligned} \tag{12}$$

with the K_j quantum numbers defined as

$$K_j = \sum_{i=1}^{j} (l_i + 2n_i), \quad n_1 = 0, \quad K \equiv K_N, \tag{13}$$

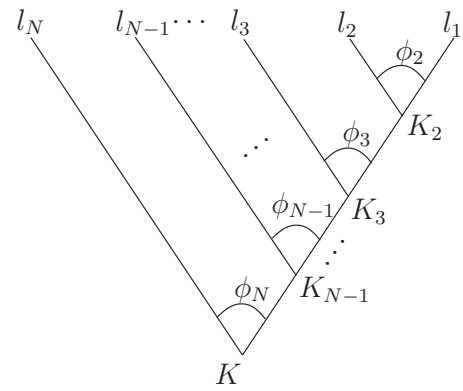

FIG. 1. Hyperspherical tree corresponding to Eq. (7).

and K also known as the grand angular momentum. The normalization factor is

$$\mathcal{N}_n^{\alpha\beta} = \sqrt{\frac{2(2n+\alpha+\beta+1)n!\,\Gamma(n+\alpha+\beta+1)}{\Gamma(n+\alpha+1)\Gamma(n+\beta+1)}}. \tag{14}$$

For the definition of the α_a, where a is either an angular momentum l_j or a quantum number K_j, one needs to introduce a hyperspherical-binary-tree structure [12], such as the one shown in Fig. 1, where the nodes are labeled by the quantum numbers a. Fixing a node a, the sub-binary tree formed by the node and by its child nodes has $\mathcal{N}_a$ nodes and $\mathcal{L}_a$ leaves, and the coefficients are defined as

$$\alpha_a = a + \mathcal{N}_a + \tfrac{1}{2}\mathcal{L}_a. \tag{15}$$

The hyperspherical tree is a graphical tool to represent the relation between the radial components of Jacobi coordinates and the hyperspherical coordinates, and to illustrate hyperangular momentum coupling schemes; the tree in Fig. 1 corresponds to the choice of hyperangles given by Eq. (7), in which Eq. (15) specializes to $\alpha_{K_j} = K_j + 3j/2 - 1$ and $\alpha_{l_j} = l_j + 1/2$.

The HH functions are normalized,

$$\int d\Omega_N (\mathcal{Y}_{[K']}(\Omega_N))^* \mathcal{Y}_{[K]}(\Omega_N) = \delta_{[K],[K']}; \tag{16}$$

moreover, the HH basis is complete:

$$\sum_{[K]} (\mathcal{Y}_{[K]}(\Omega_N))^* \mathcal{Y}_{[K]}(\Omega'_N) = \delta^{3N-1}(\Omega'_N - \Omega_N). \tag{17}$$

With the preceding definitions, the HH functions do not have well-defined total orbital angular momentum L and z projection M. It is possible to construct HH functions having well-defined values of LM by coupling the functions $Y_{l_j m_j}(\hat{x}_j)$. This can be achieved using different coupling schemes. Accordingly, we can define the following HH function:

$$\begin{aligned} \mathcal{Y}_{[K]}^{LM}(\Omega_N) = {} & \left[\prod_{j=2}^{N} {}^{(j)}\mathcal{P}_{K_j}^{\alpha_{l_j},\alpha_{K_{j-1}}}(\phi_j) \right] [Y_{l_1}(\hat{\boldsymbol{x}}_1) \\ & \otimes Y_{l_2}(\hat{\boldsymbol{x}}_2)|_{L_2} \ldots \otimes Y_{l_{N-1}}(\hat{\boldsymbol{x}}_{N-1})|_{L_{N-1}} \\ & \otimes Y_{l_N}(\hat{\boldsymbol{x}}_N)]_{LM}, \end{aligned} \tag{18}$$

having well-defined values of LM, with the particular coupling scheme in which particles (1, 2) are coupled to L_2, which in turn, with l_3, is coupled to L_3 and so on, generating $N-2$ intermediate L_i values. The set of quantum numbers $[K]$ includes the $n_2 \dots n_N$ indices of the Jacobi polynomials, the $l_1 \dots l_N$ angular momenta of the particles, and the intermediate couplings $L_2 \dots L_{N-1}$. The hyperspherical tree structure in Fig. 1 describes, as mentioned, the hyperspherical-coordinate choice of Eq. (7). However, other hyperspherical-coordinate definitions are possible, and the corresponding hyperspherical functions can be related using the $\mathcal{T}$ coefficients [15,16]. Schematically, these coefficients connect two tree structures

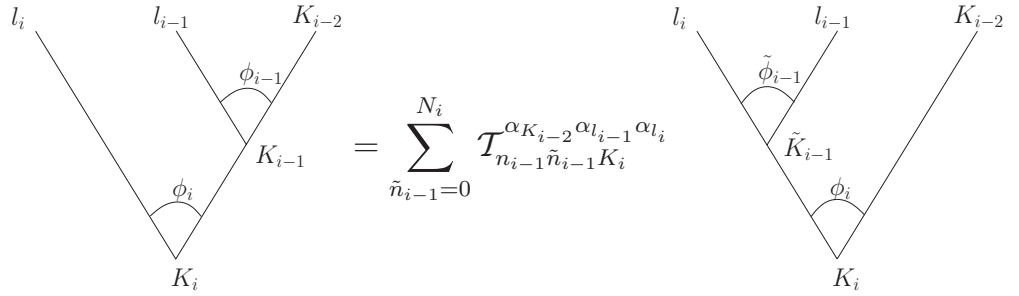

(19)

and play the same rôle of three-momenta recoupling as the $6j$ coefficients, but for the grand angular momenta. Here $K_i = K_{i-1} + l_i + 2n_i = \tilde{K}_{i-1} + l_i + 2\tilde{n}_i$. The explicit definition of the coefficients is

$$\mathcal{T}^{\alpha_{K_{i-2}}\alpha_{l_{i-1}}\alpha_{l_i}}_{n_{i-1}\tilde{n}_{i-1}K_i} = \frac{\mathcal{N}^{\alpha_{K_{i-2}}\alpha_{l_{i-1}}}_{n_{i-1}} \mathcal{N}^{\alpha_{K_{i-1}}\alpha_{l_i}}_{n_i} \binom{n_{i-1}+\alpha_{K_{i-2}}}{n_{i-1}}}{\mathcal{N}^{\alpha_{l_{i-1}}\alpha_{l_i}}_{\tilde{n}_{i-1}} \mathcal{N}^{\alpha_{K_{i-2}}\alpha_{\tilde{K}_{i-1}}}_{\tilde{n}_i} \binom{\tilde{n}_i+\alpha_{K_{i-2}}}{\tilde{n}_i}} \left(\frac{1}{2}\right)^{n_{i-1}} \frac{2\tilde{n}_{i-1}+\alpha_{l_i}+\alpha_{l_{i-1}}+1}{2^{\alpha_{l_i}+\alpha_{l_{i-1}}+1}} \frac{\tilde{n}_{i-1}!\,\Gamma(\tilde{n}_{i-1}+\alpha_{l_i}+\alpha_{l_{i-1}}+1)}{\Gamma(\tilde{n}_{i-1}+\alpha_{l_i}+1)\Gamma(\tilde{n}_{i-1}+\alpha_{l_{i-1}}+1)}$$
$$\times \int_{-1}^{1} dy\,(1-y)^{\alpha_{l_{i-1}}+n_{i-1}}(1+y)^{\alpha_{l_i}} P_{n_i}^{\alpha_{K_{i-1}}\alpha_{l_i}}(y)\, P_{\tilde{n}_{i-1}}^{\alpha_{l_{i-1}}\alpha_{l_i}}(y). \tag{20}$$

Furthermore, in Eq. (20) the integral can be rewritten as a hypergeometrical function using the following identity:

$$\int_{-1}^{1} dy\,(1-y)^{\tau}(1+y)^{\beta} P_n^{(\alpha,\beta)}(y) P_m^{(\rho,\sigma)}(y)$$
$$= \frac{\Gamma(\alpha-\tau+n)\Gamma(\beta+n+1)\Gamma(\rho+m+1)\Gamma(\tau+1)}{\Gamma(\rho+1)\Gamma(\alpha-\tau)\Gamma(\beta+\tau+n+2)} \frac{2^{\beta+\tau+1}}{m!n!}\ {}_4F_3\left[\begin{matrix}-m,\ \rho+\sigma+m+1,\ \tau+1,\ \tau+1,\ \tau-\alpha+1\\ \rho+1,\ \beta+\tau+n+2,\ \tau-\alpha-n+1\end{matrix}\right]. \tag{21}$$

For the sake of completeness, we also report the notation we use for the recoupling of three-angular momenta,

$$\left[\left[Y_{l_{i-2}}(\hat{\mathbf{x}}_{i-2})Y_{l_{i-1}}(\hat{\mathbf{x}}_{i-1})\right]_{L_{i-1}} Y_{l_i}(\hat{\mathbf{x}}_i)\right]_{L_i} = \sum_{\tilde{L}_{i-1}} T^{l_{i-2}l_{i-1}l_i}_{L_{i-1}\tilde{L}_{i-1}L_i} \left[Y_{l_{i-2}}(\hat{\mathbf{x}}_{i-2})\left[Y_{l_{i-1}}(\hat{\mathbf{x}}_{i-1})Y_{l_i}(\hat{\mathbf{x}}_i)\right]_{\tilde{L}_{i-1}}\right]_{L_i}, \tag{22}$$

where we have defined

$$T^{l_{i-2}l_{i-1}l_i}_{L_{i-1}\tilde{L}_{i-1}L_i} = (-1)^{l_{i-2}+l_{i-1}+l_i+L_i}\sqrt{2L_{i-1}+1}\sqrt{2\tilde{L}_{i-1}+1}\begin{Bmatrix} l_{i-2} & l_{i-1} & L_i \\ l_i & L_i & \tilde{L}_{i-1}\end{Bmatrix}. \tag{23}$$

Both T and $\mathcal{T}$ coefficients have particular relevance in the construction of HH functions with arbitrary permutational symmetry [8,17].

B. Rotation matrices between HH basis elements of different Jacobi coordinates

The Jacobi coordinates explicitly depend on the method of numbering the A particles. In particular, for an equal-mass system, we have selected a successive order in Eq. (3) starting from the definition of $\mathbf{x}_N = \mathbf{r}_2 - \mathbf{r}_1$. In the following we refer to this set as the reference Jacobi set. However, different choices are possibles, starting, for example, from $\mathbf{x}_N = \mathbf{r}_j - \mathbf{r}_i$, with the related HH functions depending differently on the particle variables. In general, the Jacobi coordinates can be defined from a permutation $\{p \equiv p_1 \dots p_A\}$ of the A particles, $\mathbf{r}_{p_1} \dots \mathbf{r}_{p_A}$, resulting in a redefinition of the Jacobi coordinates in which $\mathbf{r}_i$, on Eq. (3), is changed to $\mathbf{r}_{p_i}$. The associated HH functions, $\mathcal{Y}^{LM}_{[K]}(\Omega^p_N)$, are still defined by Eq. (25). The explicit indication of the index p of the

permutation allows one to trace back the dependence on the particle variables. It is a general property of the HH basis that elements constructed using a permutation p in the arrangement of the particles can be expressed as a linear combination of HH basis elements defined using some other order, both having the same grand angular quantum number. In our case, we use the HH basis constructed with the reference Jacobi set to express bases constructed with other arrangements. Accordingly, the property reads

$$\mathcal{Y}^{LM}_{[K]}(\Omega^p_N) = \sum_{[K']} \mathcal{C}^{p,LM}_{[K][K']} \mathcal{Y}^{LM}_{[K']}(\Omega_N), \tag{24}$$

where the sum runs over all quantum numbers compatible with the condition $K = K'$. As indicated, in the transformation the total angular momentum LM is conserved. For a given number of particles, N_K denotes the number of HH functions having the same value of K. Consequently, the coefficients of the transformation $\mathcal{C}^{p,LM}_{[K][K']}$ form a matrix of dimension $N_K \times N_K$. For $A = 3$ these matrix elements are the Raynal-Revai coefficients [18], whose expression is explicitly known. For $A > 3$ the coefficients cannot be given in a close form, and a few methods have been derived for their calculations [6,19–21].

Here we are interested in a particular set of coefficients relating the reference HH basis to a basis in which the orderings of two adjacent particles have been transposed. It is easy to verify that there are $A-1$ sets of Jacobi coordinates of this kind based on the following ordering of the particles: $(\mathbf{r}_1, \ldots, \mathbf{r}_A, \mathbf{r}_{A-1})$, $(\mathbf{r}_1, \ldots, \mathbf{r}_{A-1}, \mathbf{r}_{A-2}, \mathbf{r}_A), \ldots,$ $(\mathbf{r}_1, \mathbf{r}_3, \mathbf{r}_2, \ldots, \mathbf{r}_A), (\mathbf{r}_2, \mathbf{r}_1, \ldots, \mathbf{r}_A)$. The latter ordering results in a Jacobi set in which all the Jacobi vectors are equal to those of the reference set except the last one, $\mathbf{x}_N$, which is now $\mathbf{x}'_N = \mathbf{r}_1 - \mathbf{r}_2$. The other $A-2$ orderings lead to $N-1$ Jacobi sets that differ, with respect to the original Jacobi set, in the definition of two Jacobi vectors. In fact, given the transposition between particles j, $j+1$, only the Jacobi vectors $\mathbf{x}_i$ and $\mathbf{x}_{i+1}$, with $i = N - j + 1$, are different. We label them $\mathbf{x}'_i$ and $\mathbf{x}'_{i+1}$, and explicitly they are

$$\begin{aligned} \mathbf{x}'_i &= -\frac{1}{j}\,\mathbf{x}_i + \frac{\sqrt{(j+1)^2 - 2(j+1)}}{j}\,\mathbf{x}_{i+1}, \\ \mathbf{x}'_{i+1} &= \frac{\sqrt{(j+1)^2 - 2(j+1)}}{j}\,\mathbf{x}_i + \frac{1}{j}\,\mathbf{x}_{i+1}, \end{aligned} \tag{25}$$

with $i = 1, \ldots, N-1$. The corresponding moduli verify $x'^2_i + x'^2_{i+1} = x^2_i + x^2_{i+1}$. The value $i = 1$ corresponds to the transposition of the pair $(\mathbf{r}_{A-1}, \mathbf{r}_A)$, whereas the value $i = N-1$ corresponds to the transposition of the pair $(\mathbf{r}_2, \mathbf{r}_3)$. Let us call $\mathcal{Y}^{LM}_{[K]}(\Omega^i_N)$ the HH basis element constructed in terms of a set of Jacobi coordinates in which the ith and $i+1$-th Jacobi vectors are given by Eq. (25), with all the other vectors equal to the original ones (transposed basis). The case $i = N$ corresponds to the special case, mentioned before, in which all the vectors are equal except $\mathbf{x}_N$. The coefficients

$$\mathcal{A}^{i,LM}_{[K][K']} = \int d\Omega_N \left[\mathcal{Y}^{LM}_{[K]}(\Omega_N)\right]^* \mathcal{Y}^{LM}_{[K']}(\Omega^i_N) \tag{26}$$

are the matrix elements of a matrix $\mathcal{A}^{LM}_i$ that allows expression of the transposed HH basis elements in terms of the reference basis. They are a particular case of the general $\mathcal{C}^{p,LM}_{[K][K']}$ defined in Eq. (24), and therefore, the total angular momentum as well as the grand angular quantum number K is conserved in the preceding integral ($K = K'$). The coefficients $\mathcal{A}^{i,LM}_{[K][K']}$ can be calculated analytically using the T and $\mathcal{T}$ coupling coefficients and the Raynal-Revai matrix elements [6,15,16]. In fact, we have seen that only two Jacobi coordinates are changed in the construction of the transposed HH basis [see Eq. (25)]. If the two coordinates are directly coupled in both grand angular and angular space, as is the case for the pair $\mathbf{x}_1$ and $\mathbf{x}_2$, corresponding to $i = 1$, the coefficient reduces to the Raynal-Revai coefficient. Explicitly,

$$\mathcal{A}^{1,LM}_{[K][K']} = \delta_{K,K'} \left[\prod_{i=3}^{N} \delta_{l_i,l'_i} \delta_{L_{i-1},L'_{i-1}} \delta_{K_{i-1},K'_{i-1}}\right] \mathcal{R}^{K_2,L_2}_{l_2 l_1, l'_2 l'_1}, \tag{27}$$

with

$$\begin{aligned} \mathcal{R}^{K,L}_{l_2 l_1, l'_2 l'_1} = \int (\cos\phi \sin\phi)^2 d\phi\ {}^{(2)}\mathcal{P}^{l_2,l_1}_K(\phi) \int d\hat{x}_1 d\hat{x}_2 \\ \times \left[Y_{l_1}(\hat{\mathbf{x}}_1) \otimes Y_{l_2}(\hat{\mathbf{x}}_2)\right]^*_{LM}\ {}^{(2)}\mathcal{P}^{l'_2,l'_1}_K(\phi') \left[Y_{l'_1}(\hat{\mathbf{x}}'_1) \right. \\ \left. \otimes Y_{l'_2}(\hat{\mathbf{x}}'_2)\right]_{LM}, \end{aligned} \tag{28}$$

whose analytic form has been given in Ref. [18]. In Eq. (28) $\hat{\mathbf{x}}'_1, \hat{\mathbf{x}}'_2$ are the unit vectors corresponding to the coordinates defined in Eq. (25) and ϕ' is the hyperangle defined through the relation $x'_2 = \rho' \cos\phi'$, with $\rho'^2 = x'^2_1 + x'^2_2 = x^2_1 + x^2_2$. When $2 \leqslant i \leqslant N-1$, we still have a transformation between only two Jacobi coordinates, and the coefficients read

$$\begin{aligned} \mathcal{A}^{i,LM}_{[K][K']} = \left[\prod_{j=1}^{i-1} \delta_{l_j,l'_j} \prod_{k=2}^{i-1} \delta_{L_k,L'_k} \delta_{K_k,K'_k}\right] {}^{(i)}\mathcal{A}^{L_{i-1}K_{i-1},L_{i+1}K_{i+1}}_{l_i,l'_i,l_{i+1},l'_{i+1},L_iK_i,L'_iK'_i} \\ \times \left[\prod_{j=i+2}^{N} \delta_{l_j,l'_j} \prod_{k=i+1}^{N} \delta_{L_k,L'_k} \delta_{K_k,K'_k}\right], \end{aligned} \tag{29}$$

where $L_N = L$ and $K_N = K$. From the conservation of partial angular and grand angular momenta and the fact that $x^2_i + x^2_{i+1} = x'^2_i + x'^2_{i+1}$, the matrices ${}^{(i)}\mathcal{A}$ can be obtained from a three-dimensional integral. However, as shown in Ref. [16], they can be reduced to Raynal-Revai coefficients using the T and $\mathcal{T}$ coefficients to recouple the quantum numbers relative to the Jacobi variables $\mathbf{x}_i$ and $\mathbf{x}_{i+1}$. The final expression is

$$\begin{aligned} &{}^{(i)}\mathcal{A}^{L_{i-1}K_{i-1},L_{i+1}K_{i+1}}_{l_i,l'_i,l_{i+1},l'_{i+1},L_iK_i,L'_iK'_i} \\ &= \sum_{\tilde{L}_i} T^{L_{i-1}l_il_{i+1}}_{L_i\tilde{L}_iL_{i+1}}\ T^{L_{i-1}l'_il'_{i+1}}_{L'_i\tilde{L}_iL_{i+1}} \sum_{\tilde{n}_i} \mathcal{T}^{\alpha_{K_{i-1}}\alpha_{l_i}\alpha_{l_{i+1}}}_{n_i\tilde{n}_iK_{i+1}}\ \mathcal{T}^{\alpha_{K_{i-1}}\alpha_{l'_i}\alpha_{l'_{i+1}}}_{n'_i\tilde{n}_iK_{i+1}} \\ &\times \mathcal{R}^{\tilde{K}_i,\tilde{L}_i}_{l_{i+1}l_i,l'_{i+1}l'_i}, \end{aligned} \tag{30}$$

where $\tilde{K}_i = l_i + l_{i+1} + 2\tilde{n}_i$. Finally, the case $i = N$ corresponds to the transposition of particles $(1,2)$ resulting in

$\mathbf{x}'_N = -\mathbf{x}_N$ and the coefficient reduces to a simple phase factor,

$$\mathcal{A}^{N,LM}_{[K][K']} = (-1)^{l_N}\delta_{[K],[K']}. \tag{31}$$

We are now interested in obtaining the rotation coefficients between the reference HH basis and a basis in which the last Jacobi vector is defined as $\mathbf{x}'_N = \mathbf{r}_j - \mathbf{r}_i$; without losing generality, we consider $j > i$. A generic rotation coefficient of this kind can be constructed as successive products of the $\mathcal{A}^{k,LM}_{[K][K']}$ coefficients. For $j \geqslant 3$, if $\mathbf{x}_{N-j+2}$ is the last Jacobi vector in which particle j appears, at maximum $2(j-2)$ factors have to be included in the product. To see this, we start discussing the case $j = 3$, resulting in two different bases, one having the vector $\mathbf{x}'_N = \mathbf{r}_3 - \mathbf{r}_1$ and the other the vector $\mathbf{x}'_N = \mathbf{r}_3 - \mathbf{r}_2$. The rotation coefficient that relates the basis having the vector $\mathbf{x}'_N = \mathbf{r}_3 - \mathbf{r}_1$ to the reference basis is $\mathcal{A}^{N-1,LM}_{[K][K']}$, as it corresponds to the transposition of particles (2, 3). In the second case we have to consider the transpositions of particles (2, 3) and (1, 2) and the coefficient is the product between $\mathcal{A}^{N-1,LM}_{[K][K']}$ and $\mathcal{A}^{N,LM}_{[K][K']}$. Therefore, in the case $j = 3$, the rotation coefficients include at maximum the multiplication of two $\mathcal{A}$ coefficients. There are three vectors $\mathbf{x}'_N = \mathbf{r}_j - \mathbf{r}_i$ with $j = 4$. When $i = 1$ or $i = 2$, the transposition (3, 4) leads to the previous case and two and three factors are needed, respectively. For the case $\mathbf{x}'_N = \mathbf{r}_4 - \mathbf{r}_3$, the intermediate transposition (2, 3) is needed, with the consequence that the rotation coefficient includes four factors, and so on.

Defining $\mathcal{Y}^{LM}_{[K]}(\Omega^{ij}_N)$ the HH basis element constructed in terms of a set of Jacobi coordinates in which the Nth Jacobi vector is defined, $\mathbf{x}'_N = \mathbf{r}_j - \mathbf{r}_i$, the rotation coefficient relating this basis to the reference basis can be given in the following form:

$$\begin{aligned}\mathcal{B}^{ij,LM}_{[K][K']} &= \int d\Omega \left[\mathcal{Y}^{LM}_{[K]}(\Omega_N)\right]^* \mathcal{Y}^{LM}_{[K]}\left(\Omega^{ij}_N\right) \\ &= \left[\mathcal{A}^{LM}_{i_1}\cdots\mathcal{A}^{LM}_{i_n}\right]_{[K][K']}.\end{aligned} \tag{32}$$

The particular values of the indices $i_1, \ldots, i_n$, labeling the matrices $\mathcal{A}^{LM}_{i_1}, \ldots, \mathcal{A}^{LM}_{i_n}$, depend on the pair (i, j). The number of factors cannot be greater than $2(j-2)$ and it increases, at maximum, by 2 units from j to $j+1$. The matrix

$$\mathcal{B}^{LM}_{ij} = \mathcal{A}^{LM}_{i_1}\cdots\mathcal{A}^{LM}_{i_n} \tag{33}$$

is written as a product of the sparse matrices $\mathcal{A}^{LM}_i$, a property that is particularly well suited for a numerical implementation of the potential energy matrix is discussed in the next section.

III. THE POTENTIAL ENERGY MATRIX IN TERMS OF THE $\mathcal{A}$ coefficients

The potential energy of an A-body system constructed in terms of two-body interactions reads

$$V = \sum_{i<j} V(i, j). \tag{34}$$

Considering the case of a central two-body interaction, its matrix elements in terms of the HH basis of Eq. (18) are

$$V_{[K][K']}(\rho) = \sum_{i<j}\left\langle \mathcal{Y}^{LM}_{[K]}(\Omega_N)\middle|V(i, j)\middle|\mathcal{Y}^{LM}_{[K']}(\Omega_N)\right\rangle. \tag{35}$$

In each element $\langle\mathcal{Y}^{LM}_{[K]}|V(i, j)|\mathcal{Y}^{LM}_{[K']}\rangle$ the integral is understood on all the hyperangular variables and depends parametrically on ρ. Explicitly, for the pair (1, 2), it results in

$$\begin{aligned}V^{(1,2)}_{[K][K']}(\rho) &= \left\langle \mathcal{Y}^{LM}_{[K]}(\Omega_N)\middle|V(1, 2)\middle|\mathcal{Y}^{LM}_{[K']}(\Omega_N)\right\rangle \\ &= \delta_{l_1,l'_1}\cdots\delta_{l_N,l'_N}\delta_{L_2,L'_2}\cdots\delta_{L_N,L'_N}\delta_{K_2,K'_2}\cdots\delta_{K_N,K'_N} \\ &\quad\times\int d\phi_N(\cos\phi_N\sin\phi_N)^2\ {}^{(N)}\mathcal{P}^{l_N,K_{N-1}}_{K_N}(\phi_N) \\ &\quad\times V(\rho\cos\phi_N)\ {}^{(N)}\mathcal{P}^{l_N,K_{N-1}}_{K'_N}(\phi_N).\end{aligned} \tag{36}$$

Formula (36) shows that for $A > 2$ the matrix representation of $V(1, 2)$ is sparse in this basis. Using the rotation coefficients, a general term of the potential $V(i, j)$ results:

$$\begin{aligned}V^{(i,j)}_{[K][K']}(\rho) &= \left\langle \mathcal{Y}^{LM}_{[K]}(\Omega_N)\middle|V(i, j)\middle|\mathcal{Y}^{LM}_{[K']}(\Omega_N)\right\rangle \\ &= \sum_{[K''][K''']}\mathcal{B}^{ij,LM}_{[K''][K]}\mathcal{B}^{ij,LM}_{[K'''][K']}\left\langle \mathcal{Y}^{LM}_{[K]}\left(\Omega^{ij}_N\right)\right. \\ &\quad\times\left.\middle|V(i, j)\middle|\mathcal{Y}^{LM}_{[K''']}\left(\Omega^{ij}_N\right)\right\rangle.\end{aligned} \tag{37}$$

It should be noted that

$$\begin{aligned}&\left\langle \mathcal{Y}^{LM}_{[K]}(\Omega_N)\middle|V(1, 2)\middle|\mathcal{Y}^{LM}_{[K']}(\Omega_N)\right\rangle = \\ &\quad\left\langle \mathcal{Y}^{LM}_{[K]}\left(\Omega^{ij}_N\right)\middle|V(i, j)\middle|\mathcal{Y}^{LM}_{[K']}\left(\Omega^{ij}_N\right)\right\rangle,\end{aligned} \tag{38}$$

therefore Eq. (37) results in

$$\begin{aligned}V^{(i,j)}_{[K][K']}(\rho) &= \left\langle \mathcal{Y}^{LM}_{[K]}(\Omega_N)\middle|V(i, j)\middle|\mathcal{Y}^{LM}_{[K']}(\Omega_N)\right\rangle \\ &= \sum_{[K''][K''']}\mathcal{B}^{ij,LM}_{[K''][K]}\mathcal{B}^{ij,LM}_{[K'''][K']}V^{(1,2)}_{[K''][K''']}(\rho)\end{aligned} \tag{39}$$

or, in matrix notation,

$$V_{ij}(\rho) = \left[\mathcal{B}^{LM}_{ij}\right]^t V_{12}(\rho)\,\mathcal{B}^{LM}_{ij}. \tag{40}$$

The complete potential matrix energy results in

$$\sum_{ij} V_{ij}(\rho) = \sum_{ij}\left[\mathcal{B}^{LM}_{ij}\right]^t V_{12}(\rho)\,\mathcal{B}^{LM}_{ij}. \tag{41}$$

The matrices $\mathcal{B}^{LM}_{ij}$ are block matrices, with each block labeled by the grand angular momentum K. Moreover, each block is constructed as a product of the sparse matrices $\mathcal{A}^{LM}_i$ as defined in Eq. (33). In contrast, the matrix $V_{12}(\rho)$, defined in Eq. (36), couples different values of K, but it is diagonal in the quantum numbers related to particles $3, \ldots, A$.

Each term of the sum in Eq.(41) results in a product of sparse matrices, a property that allows efficient implementation of the matrix-vector product, a key ingredient in the solution of the Schrödinger equation using iterative methods.

IV. RESULTS FOR $A = 3$–6 SYSTEMS

In this section we present results for $A = 3 - 6$ systems obtained by a direct diagonalization of the Hamiltonian of the

system. The corresponding Hamiltonian matrix is obtained using the orthonormal basis

$$\langle \rho\, \Omega \,|\, m\,[K]\rangle = \left(\beta^{(\alpha+1)/2}\sqrt{\frac{m!}{(\alpha+m)!}}\, L_m^{(\alpha)}(\beta\rho)\, \mathrm{e}^{-\beta\rho/2}\right)\mathcal{Y}_{[K]}^{LM}(\Omega_N), \quad (42)$$

where $L_m^{(\alpha)}(\beta\rho)$ is a Laguerre polynomial, with $\alpha = 3N-1$ and β a variational nonlinear parameter. The matrix elements of the Hamiltonian are obtained after integrations in the ρ, Ω spaces. They depend on the indices m, m' and $[K], [K']$ as follows:

$$\langle m'\,[K']|H|\,m\,[K]\rangle = -\frac{\hbar^2\beta^2}{m}\left(T^{(1)}_{m'm} - K(K+3N-2)T^{(2)}_{m'm}\right)\delta_{[K'][K]} + \sum_{ij}\left[\sum_{[K''][K''']} \mathcal{B}^{ij,LM}_{[K][K'']}\mathcal{B}^{ij,LM}_{[K'''][K']}V^{m,m'}_{[K''][K''']}\right]. \quad (43)$$

The matrices $T^{(1)}$ and $T^{(2)}$ have an analytical form and are given in Ref. [11]. The matrix elements $V^{m,m'}_{[K][K']}$ are obtained after integrating the matrix $V_{12}(\rho)$ in ρ space (we call the corresponding matrix V_{12}). Introducing the diagonal matrix D such that $\langle [K']\,|\,D\,|[K]\rangle = \delta_{[K],[K']}K(K+3N-2)$, and the identity matrix I in K space, we can rewrite the Hamiltonian schematically as

$$H = -\frac{\hbar^2\beta^2}{m}({}^{(1)}T\otimes I + {}^{(2)}T\otimes D) + \sum_{ij}\left[\mathcal{B}^{LM}_{ij}\right]^t V_{12}\,\mathcal{B}^{LM}_{ij}, \quad (44)$$

in which the tensor product character of the kinetic energy is explicitly given. A scheme to diagonalize such a matrix is given in the Appendix.

We choose as the central potential the Volkov potential,

$$V(r) = V_R\,\mathrm{e}^{-r^2/R_1^2} + V_A\,\mathrm{e}^{-r^2/R_2^2}, \quad (45)$$

with $V_R = 144.86$ MeV, $R_1 = 0.82$ fm, $V_A = -83.34$ MeV, and $R_2 = 1.6$ fm. The nucleons are considered to have the same mass chosen to be equal to the reference mass m and corresponding to $\hbar^2/m = 41.47$ MeV fm^2. With this parametrization of the potential, the two-nucleon system has a binding energy $E_{2N} = 0.54592$ MeV and a scattering length $a_{2N} = 10.082$ fm. This potential has been used several times in the literature, making it very useful for comparing different methods [8,13,22,23]. The use of central potentials in general produces too much binding, in particular; the $A = 5$ system is bounded. Conversely, the use of the s-wave version of the potential produces a spectrum much closer to the experimental situation. This is a direct consequence of the weakness of the nuclear interaction in p waves. Accordingly, we analyze both versions of the potential, the central Volkov potential and the s-wave projected potential. The results are obtained after direct diagonalization of the Hamiltonian matrix in Eq. (43), including $m_{\max}+1$ Laguerre polynomials with a fix value of β, and all HH states corresponding to a maximum value of the grand angular momentum $K_{\max}$. The scale parameter β can be used as a nonlinear parameter to study the convergence in the index $m = 0, 1, \ldots, m_{\max}$, with $m_{\max}$ the maximum value considered. In the present analysis the convergence is studied with respect to the index $K_{\max}$; therefore, the number of Laguerre polynomials at each step, $m_{\max}+1$, is sufficiently large to guarantee independence of β of the physical eigenvalues and eigenvectors. We found that $m_{\max}+1 \approx 20$ Laguerre polynomials (with proper values of β) were sufficient for an accuracy of 0.1% in the calculated eigenvalues.

A. Symmetries of the eigenvectors

Fixing the total angular momentum and parity J^π of the state we want to describe, the diagonalization of the Hamiltonian produces eigenvectors with well-defined-permutation symmetry. Because we are using a central potential, the total angular momentum L and total spin S are good quantum numbers. Accordingly, our basis is identified by $(L, S, T)J^\pi$, where T is the total isospin of the state, and the parity corresponds to considering even or odd K values in the expansion. The eigenvalues appear either in singlets, corresponding to symmetric or antisymmetric eigenvectors, or in multiplets, corresponding to mixed-symmetry eigenvectors. The identification of the symmetry of each eigenvector can be done by applying to it the Casimir operator,

$$C(A) = \sum_{i<j} P(i,j), \quad (46)$$

where $P(i, j)$ is the permutation operator of particles (i, j). Using the results of the preceding section, the representation of the Casimir operator in the HH basis results in

$$C(A) = \sum_{i<j}\mathcal{B}^{LM}_{ij}(-1)^{L_N}\mathcal{B}^{LM}_{ij}. \quad (47)$$

As discussed in Ref. [24], this Casimir operator corresponds to the class sum $[(2)]_A$ of the group of permutation of A objects S_A, and the corresponding eigenvalues λ for the different symmetries $[\boldsymbol{\lambda}]$ are given in that reference up to $A = 5$. The eigenvectors of the Hamiltonian are also eigenvectors of this Casimir operator, therefore the application of the Casimir operator to a specific eigenvector $\Psi_n^{L^\pi}([\boldsymbol{\lambda}])$ results in

$$C(A)\Psi_n^{L^\pi}([\boldsymbol{\lambda}]) = \lambda\Psi_n^{L^\pi}([\boldsymbol{\lambda}]). \quad (48)$$

The different symmetries characterizing the spatial eigenvector are identified by λ. The physical state of A nucleons is obtained

TABLE I. $A = 3$ results for the $(L, S, T)J^\pi = (0, \frac{1}{2}, \frac{1}{2})\frac{1}{2}^+$ state using the all-wave and s-wave Volkov potential as a function of the maximum grand angular quantum number $K_{\max}$. Values for the ground-state E_0 as well as the excited-state E_1 are listed.

$K_{\max}$	all waves (MeV)		s wave (MeV)	
	E_0	E_1	E_0	E_1
20	8.4623	0.3627	8.4283	0.3618
40	8.4649	0.5181	8.4309	0.5174
60	8.4649	0.5595	8.4309	0.5589
80	8.4649	0.5773	8.4309	0.5768
100		0.5866		0.5861
120		0.5918		0.5913
140		0.5947		0.5943
160		0.5965		0.5960
180		0.5976		0.5971
200		0.5982		0.5978
240		0.5989		0.5985
280		0.5992		0.5988
320		0.5993		0.5989
SVM [22]	8.46			
Ref. [8]	8.462	0.2599		

after multiplying $\Psi_n^{L^\pi}([\boldsymbol{\lambda}])$ by the proper spin-isospin state to obtain an antisymmetric state.

B. $A = 3, 4$ systems

In Ref. [11] the binding energies $E_0(3)$ and $E_0(4)$ corresponding to the ground states of the $A = 3, 4$ systems has been studied using the Volkov potential. Here we extend the analysis to other states of the spectrum using, in addition, the s-wave version of the potential. In particular, the $A = 3$ system presents a shallow excited state. It is known that when the two-body system presents a shallow binding energy E_{2N} and a large scattering length a_{2N}, the three-body system can show a certain number of bound states close to the two-body threshold, called Efimov states (see Ref. [25], and references therein). In the present case, this behavior is a consequence of the parametrization of the Volkov potential that has been tuned to approximate the binding energy of the $A = 3$ system. In doing that, the binding energy of the $A = 2$ system turns out to be much lower than the experimental deuteron binding energy. Despite this unrealistic situation, here we are interested in studying the HH expansion for systems with $A > 4$. The analysis of the $A = 3, 4$ systems serves as a basis for establishing the different thresholds that appear in the description of those systems.

In Table I the $A = 3$ results for the state $(L, S, T)J^\pi = (0, 1/2, 1/2)1/2^+$ are given using the all-wave as well as the s-wave potential. The ground-state binding energy E_0 converges at the level of 0.1 keV, with $K_{\max} = 40$ and $m_{\max} = 24$. For the sake of comparison, the results of the stochastic variational model (SVM) from Ref. [22] and those from Ref. [8] are given in Table I. The convergence of the binding energy E_1 of the shallow state, at the same level of accuracy, necessitates a much larger basis. The maximum grand angular quantum number has been increased up to $K_{\max} = 320$ and $m_{\max} = 32$. Above $K_{\max} = 60$, only symmetric states with $l_1 = l_2 = 0$ have been considered. This very different pattern of convergence in the two binding energies, E_0 and E_1, has been observed before [26,27]. Moreover, the patterns of convergence of the all-wave and s-wave potentials are similar, as the structure of these states corresponds mostly to the particles being in a relative $l = 0$ state.

When the attraction of the two-body potential is increased, the two-body binding energy E_{2N} increases more rapidly than the E_1 energy, and at some point, the Efimov state starts to be above the two-body threshold (see, e.g., Ref. [28]). When realistic forces are used to describe the three-nucleon system there is no observation of an excited state, in agreement with the experimental situation. However, the effective range function presents a pole close to the two-body threshold [29], which can be interpreted as an Efimov-like state embedded in the continuum. When the Coulomb interaction is included, the ground-state binding energy is $E_0 = 7.7594$ MeV (all-wave potential) and $E_0 = 7.7254$ MeV (s-wave potential). In both cases the isospin components $T = 1/2$ and $3/2$ are included. With the repulsion induced by the Coulomb potential, the excited state is no longer bounded.

The $L = 0$ state of the $A = 4$ system is analyzed first. The spatially symmetric state of four nucleons can be antisymmetrized using the $S = 0$, $T = 0$ spin-isospin functions. In Table II the pattern of convergence, in terms of $K_{\max}$, is reported for the first two levels of the $(L, S, T)J^\pi = (0, 0, 0)0^+$

TABLE II. Binding energies for the $A = 4$ ground-state E_0 and the first excited-state E_1 of the $(L, S, T)J^\pi = (0, 0, 0)0^+$ state using the all-wave and s-wave Volkov potentials as a function of the maximum grand angular quantum number $K_{\max}$. In the last four columns the Coulomb interaction has been considered. For the sake of comparison, results from Refs. [8] and [22] are listed.

$K_{\max}$	all waves (MeV)		s wave (MeV)		all waves (MeV)		s wave (MeV)	
	E_0	E_1	E_0	E_1	E_0	E_1	E_0	E_1
0	28.580	3.238	28.580	3.238	27.748	2.787	27.748	2.787
10	30.278	7.509	30.116	7.445	29.456	7.039	29.292	6.976
20	30.416	8.223	30.250	8.164	29.596	7.778	29.429	7.720
30	30.418	8.463	30.252	8.403	29.599	8.035	29.431	7.976
40	30.418	8.562	30.252	8.501	29.600	8.144	29.432	8.085
SVM [22]	30.42							
Ref. [8]	30.406	8.036						

state using both versions of the Volkov potential. The ground-state binding energy E_0 converges at the level of 1–2 keV for $K_{\max} = 40$, whereas the convergence of the excited-state binding energy E_1 has been estimated at the level of 50 keV. For both potentials the excited state proves to be bounded with respect to the $3 + 1$ threshold. For the sake of comparison the results of the SVM and those from Ref. [8] are listed in Table II. To compare the results to the experimental value for the α particle, $B(^4\text{He}) = 28.30$ MeV, the last four columns in Table II list the results including the Coulomb potential between the two protons. The obtained values of 29.60 MeV (all-wave potential) and 29.43 MeV (s-wave potential) show a pronounced overbinding. This is the usual situation when central interactions are used to describe the ^{4}He nucleus and it is at variance with the case in which realistic NN forces are used. When the Coulomb potential is included the excited state appears slightly above the $3 + 1$ threshold. In the case of the all-wave potential the lowest threshold, corresponding to a p-^{3}H configuration, is at 8.465 MeV, whereas for the s-wave potential it is 8.431 MeV. The n-^{3}He thresholds are at 7.759 and 7.725 MeV, respectively. Though the convergence for E_1 was not completely achieved, the description is close to the experimental observation of a 0^+ resonance between both thresholds, centered 395 keV above the p-^{3}H threshold.

Let us consider the negative-parity $L = 1$ state. The lowest level corresponds to the [**3 1**] irreducible representation and can be antisymmetrized using the $S = 1$, $T = 0$ or $S = 0$, $T = 1$ spin-isospin functions of four nucleons. Accordingly, using a central potential, the $J^\pi = 0^-, 1^-, 2^-$ states are degenerated. The results are listed in Table III. We can observe that the all-wave potential produces a bound state at approximately 10.4 MeV from the experimental observation of a 0^- resonance 800 keV above the 0^+ resonance. Conversely, using the s-wave potential the level is unbounded. It appears at approximately 1.4 MeV above the 3+1 threshold and at approximately 1.3 MeV above the 0^+ resonance, in better agreement with the experimental situation. When the Coulomb potential between the two protons is considered, the triple degeneracy of the [**3 1**] representation breaks into three different levels, E_0, E_1, and E_2, reported in the last three columns in Table III. The first and third level are mostly $T = 0$ and can be identified with the $(J^\pi, T) = (0^-, 0)$ and $(2^-, 0)$ resonances, whereas the E_1 level is mostly $T = 1$ and can be identified with the $(1^-, 1)$ resonance, observed in the low-energy spectrum of ^{4}He [30].

TABLE III. Binding energy of the $A = 4$ lowest level having $L = 1$, using the all-wave and s-wave Volkov potentials, as a function of the maximum grand angular quantum number $K_{\max}$. In the case of the s-wave potential, when the Coulomb interaction between particles (1,2) is considered, the level splits into three sublevels, whose energies E_0, E_1, and E_2 are listed in the last three columns.

$K_{\max}$	all waves	s wave	E_0 (MeV)	E_1 (MeV)	E_2 (MeV)
1	7.965	0.387	–	–	–
3	8.411	1.975	1.639	1.440	1.374
11	10.121	5.567	5.314	5.091	4.899
21	10.373	6.642	6.456	6.276	5.955
31	10.406	7.113	6.965	6.850	6.417

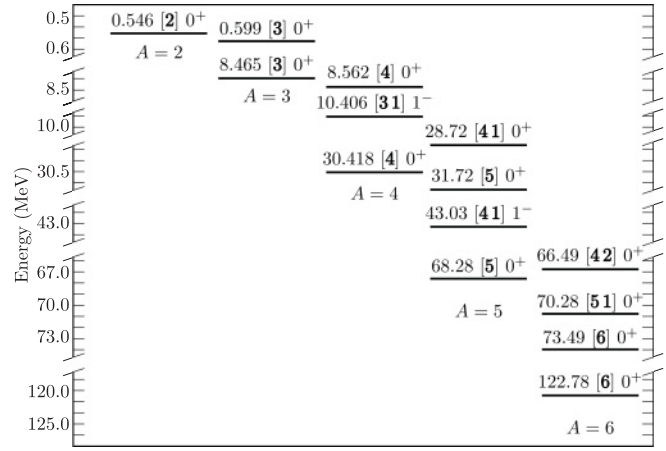

FIG. 2. Calculated levels for $A = 2$–6 using the all-wave Volkov potential.

We can conclude that besides its simplicity, the s-wave potential describes the $A = 4$ system better than the all-wave potential and, in some cases, in reasonable agreement with the experiment. The convergence of the $L = 0$ first excited state, E_1, presents some difficulties, as its energy is very close to the threshold. When the Coulomb interaction is taken into account this level moves to the continuum and it appears as a resonance between the two $3 + 1$ thresholds, in agreement with the experimental data. To accurately extract its position and width, the present method can be combined with the procedure developed, for example, in Ref. [31]. The computed states for $A = 3, 4$ are collected in Figs. 2 and 3.

C. $A = 5, 6$ systems

In the case of systems with $A > 4$ the spatially symmetric state cannot be antisymmetrized using the corresponding spin-isospin functions. Therefore, it is interesting to study the symmetry of the different levels in the $A = 5$ system

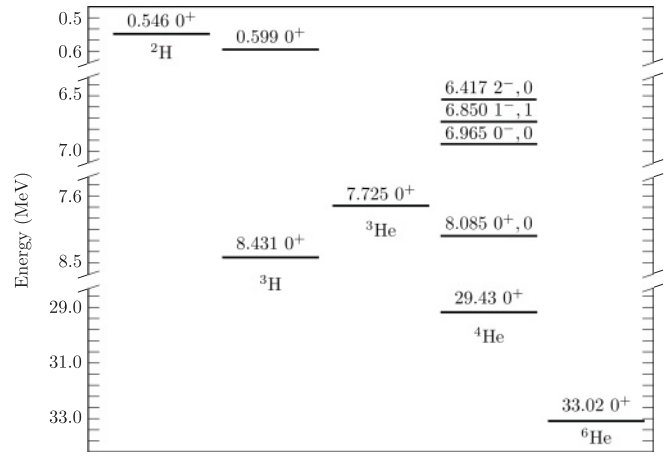

FIG. 3. Calculated levels for $A = 2, 3, 4$, and 6, using the s-wave Volkov potential with the inclusion of the Coulomb interaction for He isotopes. In this case the $A = 5$ system is unbounded.

TABLE IV. $A = 5$ binding energies of the first three levels of the $L = 0$ state, belonging to the indicated irreducible representation [λ], as a function of $K_{\max}$. The size of the HH basis N_{HH} is also indicated.

$K_{\max}$	$N_{\rm HH}$	E_0 (MeV) [**5**]	E_1 (MeV) [**5**]	E_2 (MeV) [**4 1**]
0	1	64.864	24.472	–
2	10	64.864	24.472	20.160
4	55	65.958	28.411	22.043
6	220	66.893	29.517	24.415
8	714	67.713	30.228	25.568
10	1 992	68.008	30.587	26.459
12	4 950	68.177	30.927	27.043
14	11 220	68.239	31.152	27.515
16	23 595	68.264	31.357	27.862
18	46 618	68.274	31.509	28.143
20	87 373	68.278	31.628	28.371
22	156 520	68.279	31.715	28.560
24	269 620	68.280	31.779	28.719

when the nonsymmetrized basis is used. For the positive-parity $L = 0$ state, using the Volkov potential, the deepest two levels correspond to a completely symmetric state (the irreducible representation of S_5 [**5**]). The third level belongs to the irreducible representation of S_5 [**4 1**]; it can be anti-symmetrized using the $A = 5$ spin-isospin functions having $S = 1/2$, $T = 1/2$, therefore it represents the lowest level of the $(L, S, T)J^\pi = (0, 1/2, 1/2)1/2^+$ state of five nucleons. The convergence of these three states in terms of $K_{\max}$ is reported in Table IV. The first two levels, representing bosonic bound states, present a good convergence with K (in particular, the deepest level). The [**4 1**] state is not bounded, in agreement with the fact that the $A = 5$ nucleus does not exist. Its energy turns out to be above the threshold of 30.42 MeV describing an ^{4}He nucleus plus a fifth nucleon far away (here the Coulomb interaction has not been included). For the three levels, their stability as a function of the nonlinear parameter β is shown in Fig. 4.

The negative-parity $L = 1$ state corresponds to the $(L, S, T)J^\pi = (1, 1/2, 1/2)1/2^-$ and $(1, 1/2, 1/2)3/2^-$ states, which are degenerate using the Volkov potential. Its deepest level belongs to the [**4 1**] representation. In Table V the convergence of this level is shown in terms of $K_{\max}$ for the all-wave potential, as well as its s-wave reduction. The table shows that the all-wave potential predicts a very deep bound state, at 43.03 MeV, whereas the s-wave reduction does not. Using the s-wave potential, the $A = 5$ system is unbounded, in agreement with the experimental observation. For these two levels, their stability as a function of the nonlinear parameter β is shown in Fig. 4 as the solid line (all waves) and long-dashed line (s wave), respectively. In the last three columns in Table V, the three levels obtained considering the s-wave Volkov potential plus the Coulomb interaction between two protons are listed. The inclusion of the Coulomb interaction breaks the degeneracy of the quartet [**4 1**] state, producing three different states that can be identified by the residual $S_2 \otimes S_3$ symmetry of the two-proton and three-neutron subsystems. The two lowest states, E_0 and

TABLE V. $A = 5$ binding energies of the deepest $L = 1$ state, as a function of $K_{\max}$, using the all-wave and s-wave Volkov potentials. In the last three columns the Coulomb potential has been summed to the s-wave Volkov potential. The size of the HH basis $N_{\rm HH}$ is also indicated.

$K_{\max}$	$N_{\rm HH}$	all waves	s wave	E_0	E_1	E_2
1	4	39.635	21.874	21.370	21.119	–
3	40	40.001	24.317	23.854	23.604	23.524
5	220	41.022	26.053	25.618	25.367	25.251
7	876	41.785	26.923	26.505	26.258	26.116
9	2 820	42.384	27.546	27.140	26.896	26.736
11	7 788	42.682	27.971	27.574	27.333	27.160
13	19 140	42.868	28.297	27.908	27.669	27.485
15	42 900	42.952	28.521	28.140	27.903	27.710
17	89 232	42.996	28.693	28.320	28.084	27.882
19	174 460	43.017	28.823	28.457	28.223	28.011
21	323 752	43.027	28.924	28.562	28.331	28.110
23	574 600	43.032	29.005	28.647	28.417	28.189
SVM		43.00				
HH [8]		42.383				

E_1, belong to the $[\mathbf{1}^2] \otimes [\mathbf{3}]$ and $[\mathbf{2}] \otimes [\mathbf{3}]$ representations of $S_2 \otimes S_3$ and cannot be antisymmetrized with respect to the three neutrons. The third level, E_2, is a doublet state belonging to the $[\mathbf{2}] \otimes [\mathbf{2\ 1}]$ representation, and it can be antisymmetrized, with the spin state of the two protons having $S_p = 0$ and the spin state of the three neutrons having $S_n = 1/2$. Physically this state is describing a scattering state between a neutron and an α particle in $J^\pi = 1/2^-$ and $3/2^-$. In the present study we are limiting the description to bound states; however, using the method described in Ref. [32], it would be possible to compute phase shifts using the $L = 0, 1$ bound-like states. The extension of the method to describe scattering states is in progress.

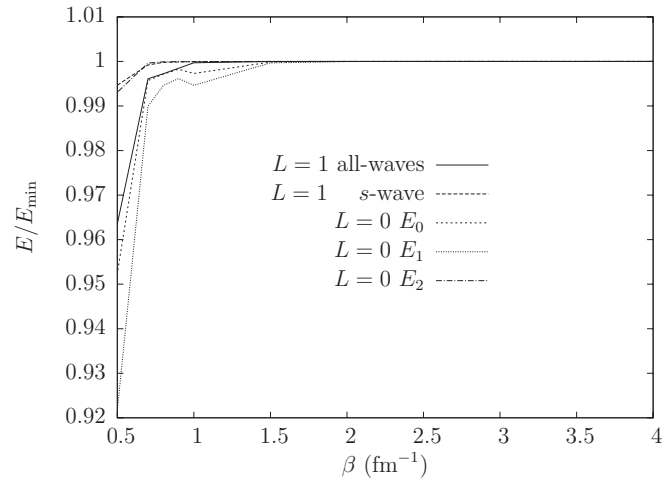

FIG. 4. $A = 5$, $L = 0$ levels listed in Table IV, denoted E_0, E_1, and E_2, and the $L = 1$ levels listed in Table V, denoted "all waves" and "s wave," normalized to the respective minimal energy $E_{\rm min}$, are shown as functions of the nonlinear parameter β, at $K_{\max} = 16$ ($L = 0$ levels) and $K_{\max} = 17$ ($L = 1$ levels).

TABLE VI. $A = 6$ binding energies of the first four levels of the $L = 0$ state, using the Volkov potential, belonging to the indicated irreducible representation [**λ**], as a function of $K_{\max}$. E_3^s indicates the binding energy of the lowest [**4 2**] state using the s-wave Volkov potential, and E_3^{sc} is the binding energy of the [**2**] ⊗ [$\mathbf{2}^2$] state, once the Coulomb interaction has been included. The size of the HH basis $N_{\rm HH}$ is also indicated.

$K_{\max}$	$N_{\rm HH}$	E_0 (MeV) [**6**]	E_1 (MeV) [**6**]	E_2 (MeV) [**5 1**]	E_3 (MeV) [**4 2**]	E_3^s (MeV) [**4 2**]	E_3^{sc} (MeV) [**2**] ⊗ [$\mathbf{2}^2$]
0	1	117.205	64.701	–	–	–	–
2	15	117.205	64.701	62.513	61.142	24.793	24.064
4	120	118.861	69.450	64.277	62.015	28.791	28.016
6	680	120.345	70.544	66.268	63.377	30.723	29.935
8	3 045	121.738	71.443	67.280	64.437	31.645	30.851
10	11 427	122.317	71.923	68.371	65.354	32.244	31.446
12	37 310	122.597	72.477	69.029	65.886	32.708	31.908
14	108 810	122.711	72.822	69.531	66.201	33.075	32.275
16	288 990	122.752	73.101	69.842	66.360	33.358	32.558
18	709 410	122.768	73.284	70.051	66.437	33.561	32.762
20	1 628 328	122.774	73.407	70.189	66.474	33.710	32.912
22	3 527 160	122.776	73.485	70.283	66.491	33.814	33.017
SVM					66.25		

In the case of the $A = 6$ system we concentrate the analysis on the $(L, S, T)J^\pi = (0, 0, 1)0^+$ and $(0, 1, 0)1^+$ states. Using a central potential, and disregarding the Coulomb interaction, these two states are degenerate. Including the Coulomb interaction between two protons, the first state has the quantum numbers of ^{6}He. A direct diagonalization of the six-body Hamiltonian using the nonsymmetrized HH basis, with the Volkov potential, produces a spectrum in which the first two levels belongs to the [**6**] irreducible representation of S_6. The third level belongs to the [**5 1**] representation, whereas the fourth level belongs to the [**4 2**] representation, and it is the first one that can be symmetrized using the $A = 6$ spin-isospin functions having $S = 0$, $T = 1$ or $S = 1$, $T = 0$. The convergence pattern of these four levels in terms of $K_{\max}$ are listed in Table VI, indicated by E_i, $i = 0, \ldots, 3$. Similarly to the $A = 5$ case, the Volkov potential acting in all waves predicts high binding energies. In particular, the binding energy of the physical state turns out to be ≈67 MeV. Using the s-wave potential, the much more reasonable value of ≈34 MeV is obtained for this level. The corresponding convergence is shown in the last column in Table VI, indicated by E_3^s. It should be noted that in the computation of the spectrum using the s-wave potential, E_3^s is no longer the fourth level. Other levels belonging to the [**6**] and [**5 1**] representation gain more energy than the [**4 2**] level, making its correct identification difficult. However, it is possible to restrict the search of the eigenvectors to those having a particular symmetry using a symmetry-adapted Lanczos method [14] (a description of the iterative method used is given in the Appendix). Essentially, starting with a vector having the desired symmetry, after each iteration of the matrix-vector product, the new vector is projected onto the subspace of the selected symmetry. Following Ref. [14], an intermediate purification step is also implemented. This method has the characteristic of finding eigenvalues corresponding to eigenvectors of one particular symmetry, simplifying the search procedure and the identification of the eigenvectors.

When the Coulomb interaction between two protons is considered, the degeneracy of the [**4 2**] level (of dimension 9) is broken and four different states appear. It is possible to identify the physical state by looking at the symmetry of the four neutrons. One of the states belongs to the [**4**] representation, two belong to the [**3 1**] representation, and the last one belongs to the [$\mathbf{2}^2$] representation of S_4. The latter state is the only one that can be antisymmetrized using the spin functions of four neutrons having $S_n = 0$. Moreover, the proton state is spatially symmetric and therefore can be antisymmetrized with the spin function $S_p = 0$, making a total $S = 0$ state. The convergence of this state is reported in the last column in Table VI. It should be noticed that this state is embedded in a very dense spectrum. To follow this state the projected Lanczos method has been used. The vector, after each matrix vector product, has been projected on antisymmetric states between particles (3,4) and particles (5,6). In this way the level belonging to the [**2**] ⊗ [$\mathbf{2}^2$] representation of $S_2 \otimes S_4$ turns out to be the lowest one. The results obtained for the different levels are collected in Figs. 2 and 3.

V. CONCLUSIONS

In this work we have developed a technique devoted to describing bound states in an A-body system without imposing a particular requirement owing to the intrinsic statistic of the particles. However, the final aim of the method is to find wave functions that fulfill this requirement.

Starting with the nonsymmetrized HH basis set, we have diagonalized the Hamiltonian of the A-body system using that basis at fixed values of K. We have observed that the eigenvectors reflect the symmetries present in the Hamiltonian, and in particular, if the system is composed of identical particles, the eigenvectors belong to the different irreducible representations of the permutation group of A objects, S_A. Using a Casimir operator, it was possible to identify those eigenvectors having the required symmetry of the system

and, accordingly, study the convergence (in terms of K) of the corresponding eigenvalues. The direct use of the nonsymmetrized HH basis has important consequences from a technical point of view. The basis is much larger than the one limited to a subspace having a particular symmetry. However, it should be noted that a system of nucleons includes spatial, spin, and isospin degrees of freedom, all of them coupled by the NN potential, with the consequence that different spatial symmetries are present in an A-nucleon wave function. Although the construction of HH basis elements having different spatial symmetries is possible (see, e.g., Ref. [8]), the necessity of including the different symmetries in the description enlarges the dimension of the basis and makes it comparable to the case in which the nonsymmetrized basis is used. This is particularly important when one wants to consider the description of the small components of the wave function induced by symmetry-breaking terms in the potential, as, for example, high isospin components.

The method presented here is based in a particular implementation of the potential energy matrix constructed as a sum of products of sparse matrices. This allows efficient use of iterative algorithms in which the matrix-vector product is a key element. However, the iterative methods are well suited to calculation of the deepest levels of the spectrum. In our formulation, owing to the presence of different symmetries, the physical states can appear very high in the spectrum or in a zone with a high density of levels. In this case we found it very convenient to use the symmetry-adapted Lanczos method [14]. Using the particular form of the permutation operator $P(i, j)$ in terms of the sparse matrices [see Eq. (47)], it was possible to project the vector in the iterative procedure to be antisymmetric in selected pairs of particles. In this way the desired symmetry becomes the lowest state of the spectrum. Although this mechanism is not as fast as searching for the true lowest state of the complete spectrum, it is much faster than searching for certain numbers of levels in a high position in the spectrum.

We should also stress that the sparse matrices ${}^{(i)}\mathcal{A}$ defined in Eq. (30) have the property of being constructed as products of the angular T coefficients, the tree $\mathcal{T}$ coefficients, and the Raynal-Revai coefficients. Whereas the latter couple quantum numbers belonging to the $[K]$ and $[K']$ sets, the T and $\mathcal{T}$ coefficients perform a recoupling of quantum numbers inside $[K]$ or $[K']$. Moreover, the Raynal-Revai coefficients $\mathcal{R}^{K,L}_{l_2 l_1, l_2' l_1'}$ couple quantum numbers belonging to three particles [see Eq. (28)]. As the number of particles A increases, more values of the quantum numbers K, L are accessible, and this makes the size of the ${}^{(i)}\mathcal{A}$ matrices increase, though slowly, with the number of particles A. Furthermore, going from a system with A particles to one with $A+1$, the number of potential terms increases by A and the number of factors in the matrix $\mathcal{B}^{LM}_{ij}$ of Eq. (33) increases, at most, by the same quantity. Although the overall number of states grows exponentially, the computational effort increases roughly linearly with A, and this fact makes feasible the application of the method for increasing values of A, as has been demonstrated in the present work. Our expectation is that the present technique can be extended to treat systems up to $A = 8$. The calculations presented here were obtained using a sequential code. We expect that an opportune parallelization of the code (which is under study) will increase the potentiality of the method.

We have limited the analysis to consideration of a central potential, the Volkov potential, used several times in the literature. Though the use of a central potential leads to an unrealistic description of the light nuclei structures, the study has served to analyze the characteristics of the method: the capability of the diagonalization procedure to construct the proper symmetry of the state and the particular structure, in terms of products of sparse matrices, of the Hamiltonian matrix. The success of this study makes feasible the extension of the method to treat interactions depending on spin and isospin degrees of freedom as the realistic NN potentials. A preliminary analysis in this direction has been done [33]. In this respect, it is important to note that the information of the potential is given in the matrix V_{12} defined in Eq. (36). Once this matrix is given, the method remains the same, with the basis enlarged to include spin and isospin degrees of freedom if required. Using the Volkov potential we have shown that it is possible to identify all the physical states and the corresponding thresholds in order to interpret the level as being bounded or belonging to the continuum. Furthermore, the results obtained using the Volkov potential up to $A = 6$ compare well with those using other techniques. A few characteristics of the $A = 3 - 6$ systems using the Volkov potential are the following. Owing to its particular parametrization a shallow state appears in the $A = 3, 4$ systems when the Coulomb interaction is not considered. In the $A = 3$ system this state has the characteristics of an Efimov state. When the Coulomb interaction is considered these states move to the continuum. The Volkov potential acting in all waves produces high binding energies as A increases. Accordingly we have included in the analysis the s-wave version of the potential. In agreement with the experimental observations, this version predicts, in reasonable positions, $A = 4$ 0^+ and 0^- resonances and no bound states in the $A = 5$ system. It also predicts reasonable binding energies in the $A = 6$ system. The extension of the method to consideration of realistic potentials is in progress.

APPENDIX

The diagonalization of the Hamiltonian is obtained by means of an iterative algorithm that requires only the action of the Hamiltonian matrix on a given vector. We used the Lanczos algorithm in the version invented by Cullum and Willoughby [34], which is particularly sparing of memory use. In principle, the iterative procedure should preserve the permutation symmetry of the input vector, as the Hamiltonian commutes with the group elements. However, the round-off errors generate components also in the other irreducible representations. To circumvent this problem, we have used a symmetry-adapted Lanczos developed in Ref. [14] in which a projection operator is applied after each iterative step. Starting from a random initial vector, in the usual Lancsoz recurrence formula

$$\beta_{i+1}\boldsymbol{v}_{i+1} = H\boldsymbol{v}_i - \alpha_i\boldsymbol{v}_i - \beta_i\boldsymbol{v}_{i-1}, \tag{A1}$$

the product $H\boldsymbol{v}_i$ is replaced by $P^{[\widehat{\lambda}]}H\boldsymbol{v}_i$, where $P^{[\widehat{\lambda}]}$ is a projector on a subspace with a nonzero intersection with the

irreducible representation [**λ**] and a zero intersection with the irreducible representations of lower-eigenvector symmetries. A purification step is also performed in which the product $\beta_{i+1}\boldsymbol{v}_{i+1}$ is replaced with $P^{[\widehat{\lambda}]}\beta_{i+1}\boldsymbol{v}_{i+1}$.

As an example in the $L = 0$ sector of the $A = 6$ system, we are interested in states belonging to the irreducible representation [**4 2**]. To eliminate lower states belonging to the irreducible representations [**6**] and [**5 1**], we have used the projector

$$P^{[\widehat{4\,2}]} = A_{12} \cdot A_{34}, \tag{A2}$$

given as the product of the antisymmetrization operator A_{12} with respect to particles (1, 2) and of the antisymmetrization operator A_{34} with respect to particles (3, 4). The two antisymmetrization operators have the following expression in terms of the $\mathcal{A}_i$ matrices (the superscript L, $M = 0, 0$ is understood):

$$A_{12} = \tfrac{1}{2}(1 - \mathcal{A}_5) \tag{A3}$$

and

$$A_{34} = \mathcal{A}_4\mathcal{A}_3\mathcal{A}_4\,\frac{1 - \mathcal{A}_5}{2}\,\mathcal{A}_4\mathcal{A}_3\mathcal{A}_4. \tag{A4}$$

[1] S. C. Pieper, K. Varga, and R. B. Wiringa, Phys. Rev. C **66**, 044310 (2002).
[2] P. Navrátil, V. G. Gueorguiev, J. P. Vary, W. E. Ormand, and A. Nogga, Phys. Rev. Lett. **99**, 042501 (2007).
[3] A. Kievsky *et al.*, Phys. Rev. C **58**, 3085 (1998).
[4] R. Lazauskas, J. Carbonell, A. C. Fonseca, M. Viviani, A. Kievsky, and S. Rosati, Phys. Rev. C **71**, 034004 (2005).
[5] H. Kamada *et al.*, Phys. Rev. C **64**, 044001 (2001).
[6] A. Novoselsky and J. Katriel, Phys. Rev. A **49**, 833 (1994).
[7] A. Novoselsky and N. Barnea, Phys. Rev. A **51**, 2777 (1995).
[8] N. Barnea, Phys. Rev. A **59**, 1135 (1999).
[9] M. Fabre de la Ripelle and J. Navarro, Ann. Phys. **123**, 185 (1979).
[10] N. K. Timofeyuk, Phys. Rev. C **78**, 054314 (2008).
[11] M. Gattobigio, A. Kievsky, M. Viviani, and P. Barletta, Phys. Rev. A **79**, 032513 (2009).
[12] N. Ya. Vilenkin, G. I. Kuznetsov, and Ya. A. Smorodinskii, Sov. J. Nucl. Phys. **2**, 645 (1966).
[13] M. Viviani, A. Kievsky, and S. Rosati, Phys. Rev. C **71**, 024006 (2005).
[14] X.-G. Wang and T. Carrington Jr., J. Chem. Phys. **114**, 1473 (2001).
[15] M. S. Kil'dyushov, Yad. Fiz. **15**, 197 (1972) [Sov. J. Nucl. Phys. **15**, 113 (1972)].
[16] M. S. Kil'dyushov, Yad. Fiz. **16**, 217 (1972) [Sov. J. Nucl. Phys. **16**, 117 (1973)].
[17] N. Barnea and A. Novoselsky, Ann. Phys. **256**, 192 (1997).
[18] J. Raynal and J. Revai, Nuovo Cimento A **68**, 612 (1970).
[19] R. Krivec and V. B. Mandelzweig, Phys. Rev. A **42**, 3779 (1990).
[20] M. Viviani, Few-Body Syst. **25**, 177 (1998).
[21] V. D. Efros, Few-Body Syst. **19**, 167 (1995).
[22] K. Varga and Y. Suzuki, Phys. Rev. C **52**, 2885 (1995).
[23] N. K. Timofeyuk, Phys. Rev. C **65**, 064306 (2002).
[24] A. Novoselsky and J. Katriel, Phys. Rev. C **51**, 412 (1995).
[25] E. Braaten and H.-W. Hammer, Phys. Rep. **428**, 259 (2006).
[26] P. Barletta and A. Kievsky, Few-Body Syst. **45**, 25 (2009).
[27] P. Barletta, C. Romero-Redondo, A. Kievsky, M. Viviani, and E. Garrido, Phys. Rev. Lett. **103**, 090402 (2009).
[28] P. Barletta and A. Kievsky, Phys. Rev. A **64**, 042514 (2001).
[29] A. Kievsky *et al.*, Phys. Lett. B **406**, 292 (1997).
[30] D. R. Tilley, H. R. Weller, and G. M. Hale, Nucl. Phys. A **541**, 1 (1992).
[31] H. Witała and W. Glöckle, Phys. Rev. C **60**, 024002 (1999).
[32] A. Kievsky, M. Viviani, P. Barletta, C. Romero-Redondo, and E. Garrido, Phys. Rev. C **81**, 034002 (2010).
[33] M. Gattobigio, A. Kievsky, M. Viviani, and P. Barletta, Few-Body Syst. **45**, 127 (2009).
[34] J. K. Cullum and R. A. Willoughby, J. Comput. Phys. **44**, 329 (1981).